

# The Effect of P-Wave Propagation on the Seismic Behavior of Steel Pipelines

Amin Ghaznavi Oskouei<sup>1\*</sup>, Asghar Vatani Oskouei<sup>1</sup>

RESEARCH ARTICLE

Received 07 August 2016; Accepted 08 April 2017

## Abstract

*Underground structures perceived as one the most vital infrastructures, which include a variety of tunnels, subway lines, gas, oil and water pipe. Plenty of studies devoted to the investigation of the effect of wave propagation method on the seismic behavior of steel pipelines. It should be mentioned that analyses have been carried out on both clayey and sandy soil with different propagation speed in each of them. The aim of this research is the investigation of the effect of longitudinal p-wave propagation method on the amount of nonlinear strains of pipeline with different way such as Pipe and Psi element or 2D modelling of soil. It became evident that the amounts of Maximum tension strain produced in the pipe have the maximum difference, equaling 3.4 per cent. In addition, it investigates the effect of frequency of input motion on nonlinear strains and the effect of frequency content in the results.*

## Keywords

*Continues Steel pipeline, sinusoidal wave, time history analyses, soil-structure interaction, and longitudinal p-wave propagation*

## 1 Introduction

The gas and oil pipelines are one of the most vulnerable existing infrastructures, because as the nature of transmitting oil and gas dictates, the smallest fraction of imposed damage can lead to numerous problems for the environment as well as the structures surrounding these pipelines. Also, given the long length of pipelines, there is a high possibility of these pipelines crossing and intersecting the faults. This intersection of pipeline with the fault has been investigated by many researchers [1] to [3]. Datta et al. examined prior research on the impact of the earthquake on the pipeline [3]. It was found that although much research has been done on the effects of faults on pipelines, but the impact of random vibration and earthquake on pipelines has been less studied [3]. Pipelines can pass different angles of various faults. Various studies have examined the impact of normal faults [4] to [6]. Karamitros et al. analytical and numerical abundance of research conducted on the pipeline and found that the regulation values of strain and stress at the intersection of faults with numerical and analytical values are a good match [5], [6]. Kouretzis et al examined the effect of P waves on the tunnels and discovered hoop stress when dealing with P waves, are much more than when dealing with S waves [7], [8]. Sedarat et al. also found similar results [9]. In all the above cases one type of Soil used and the effect of changes in soil type were not studied [9]. The effect of reverse faults have also been studied [10], [11]. Rahim-Zadeh et al. examined the effect of reverse faults on the seismic behaviour of the pipeline's [12]. It was found that although the values developed in the pipeline in the different locations is acceptably similar to ALA relations, but the amount of lift bending forces over the amount of ALA [12]. Then it was expanded to include the analytical equations for different lengths of pipe, fault and the impact angle of pipe [6], [13]. Until this time not any buried pipelines which crossing the faults have suffered huge damages [9] to [16]. It also became evident that because of the waves propagating in the soil area around the pipeline. Saberi et al. examined the effect of wave propagation on curved pipes [14], [15]. It was found that the highest levels of axial strain caused by the angle of 135 degrees in the pipeline and the axial strain values at 90 degrees was less than the

<sup>1</sup>Department of Civil Engineering  
Shahid Rajaei Teacher Training University  
Tehran, Lavizan, Shabanlou, Iran

\* Corresponding author's email: [a.ghaznavi@srttu.edu](mailto:a.ghaznavi@srttu.edu)

angle of 135 degrees [14]. Kouretzis et al studied the effect of two-dimensional Rayleigh waves [16]. It was revealed that Rayleigh waves cause more axial strain and reduce the amount of hoop strain is compared with S wave [16]. The effect of wave propagation stemming from the explosion was investigated as well [17]. Moreover, diverse methods of modelling wave propagation in structures were also investigated [18] to [24]. One of these methods was the use of spring to model the soil around the pipe [18], [19]. To evaluate the effect of wave propagation in the pipe network of nuclear power plants (which often have different boundary conditions at the ends of the pipes) asynchronous analysis was performed [20]. Yazdi et al. studied the effect of absorbing boundary condition on wave propagation [22]. For modelling pipe-soil interaction nonlinear spring were used [14], [15], and [24]. Regarding the issue of wave propagation in modelling, we should model the length of the pipe to mitigate the effect of the end of the pipe on analysis results. Hosseini et al. [25] have calculated the minimum length of the pipe based on the soil type around the pipe. The main damages imposed on the oil and gas transmission pipelines occur at the time of an earthquake affected by waves. Other researches have been conducted by Roudsari et al. to investigate the seismic behavior of GRP pipelines. Roudsari et al. embarked on the laboratorial analysis of the pipe as well as the numerical analysis of the behavior of GRP pipeline in sandy and clayey soil. The purpose of this article is to investigate the effect of axial P-wave. It should be mentioned that the bending of metal pipes and GRP has been investigated by Roudsari et al. [25]. Nonetheless, it can be supposed that structures located in areas 2 or 5 times more than the focal depth are affected by the body waves and in structures located in areas beyond 5 times more than the focal depth are dominated by surface waves. O'Rourke et al. [27] have presented graphs for changes in RL wave speed in layered soil profile. Among the surface waves only RL waves are taken into consideration to study the effect of wave propagation on the buried pipes because Love waves will lead to the bending strain in pipes which is of importance for usual diameters, whereas longitudinal component of RL waves is parallel to the propagation which leads to axial strain in the pipe parallel to the wave propagation. Since RL waves belong to the surface waves and are propagated at the land level, their apparent propagation speed at the land level is the same as their propagation speed. At the same layer with the same shear wave speed in depth, the speed of RL wave is slightly less than that of shear wave. But in normal soil layers in which the soil stiffness increases along with depth, the RL wave propagation speed depends on the changes in shear wave speed in depth as well as the frequency in spite of the body wave. Since the bending strain is not important when it comes to the propagation of axial-seismic waves in straight pipelines, only axial strains in the pipe are important and are affected by this. The aim of this research is the investigation of the effect of P-waves on the amounts of strain in the pipes.

## 1.1 The boundaries

When it comes to static analyses, the use of defined boundaries with a short distance from the structure can provide the required accuracy. The application of this boundary is not suitable for dynamic analyses due to the reflection of radiation waves as well as the overlooking of radiation damping. Although, in this case, the use of big dimensions for the bed together with the materials' damping can fulfill the supposition of the radiation waves not returning to the boundary, this approach has its own particular problems because of the need for time-consuming calculations despite the improvements in calculating velocity in the current era [28]. The radiation damping in the limited dimensions of the soil is provided using artificial absorbed boundaries. The nature of these boundaries is the absorption of energy of radiation waves to themselves. Many researches have been carried out about the performance of absorbed boundaries. Lysmer and kuhlemeyer [29] in 1969 suggested the viscous absorbed boundaries consisting of artificial boundary condition. The coefficients of above dampers are evaluated are derived based on the theory of one-dimensional propagation of the wave. The damper tangential and perpendicular to the surface are defined based on the velocity of shear and longitudinal waves respectively. These coefficients are provided in eq. (1). In this equation,  $\rho$  is the density of the bed materials,  $A$  is the effective area of the element in the location of boundary,  $c$  is the velocity of longitudinal wave and  $C_s$  is the velocity of shear wave.

$$\begin{aligned} C_T &= \rho c_s A \\ C_N &= \rho c_p A \end{aligned} \quad (1)$$

After Lysmer and kuhlemeyer, for two decades, researchers have provided numerous approaches [30 to 33] to model the proposed absorbed boundaries. Kausel in 1988 showed that all above approaches are based on the similar mathematical basis and therefore, their absorbing accuracy is more or less at the same level [34].

Deeks and Randolph [35] in 1994 introduced viscous elastic boundaries for the issues of radius plate strain. This boundary for shear waves includes spring and damper and for longitudinal waves includes spring, damper and lumped mass. It has been observed that the accuracy of this boundary is more than that of viscous boundaries presented by Lysmer. Deeks and Randolph presented the coefficients of the boundary based on the radius of the perimeter while supposing the area to be in the form of radius Liu and Du [36] in 2006 extended the viscous elastic boundary provided by Deeks and Randolph. In this research, only spring and damper are employed in every direction and the lumped mass is eliminated. Also, according to table 1, the corrected coefficients are presented in terms of the use of the presented boundaries in rectangle – shaped areas. Eq. (2) indicates the coefficients of spring and damper for different directions. In these equations, directions 1 and 2 are tangential direction, and 3 is normal direction of the surface.

Coefficients of R is equal to the depth of the model. The correction coefficients of  $\alpha$  are presented in table 1. Coefficients of  $G$  and  $A$  are the shear modulus of bed materials and the effective area of element in the location of boundary respectively. The boundaries provided by Liu and Du are only presented for linear bed and the stimulation internal excitation.

$$K_1 = K_2 = \frac{\alpha_T G}{R} A, \quad K_3 = \frac{\alpha_N G}{R} A \quad (2)$$

$$C_1 = C_2 = \rho c_s A, \quad C_3 = \rho c_p A$$

**Table 1** The correction coefficients of viscous elastic boundaries in rectangle – shaped areas.

Correction factor	Acceptable range	Suggested factor
$\alpha_N$	1.0~2.0	1.33
$\alpha_T$	0.5~1.0	0.67

It is necessary to mention that the advanced viscous elastic boundaries with various degrees including spring, damper, a series of mass and damper were presented by Du and Zhao in 2009 [37]. Li and Song in 2013 [38] present series of mass and damper for dry and saturated areas having radius coordination. One of the drawbacks of these boundaries is their complexity and application only in models with radius coordination. Furthermore, over the past two decades, new boundaries have been proposed to absorb the reflecting waves under the name of completely adjusted layers [39, 40] and have been employed in various studies [41, 42]. Despite the fact that they are more applicable than the previous approaches, they have not been able to achieve a good name and reputation yet as far as practical issues are concerned, due to the inherent complexities as well as the restrictions in terms of applying them in some seismic issues. In addition to these boundaries, Guddati and Tassoulas in 2000 [43] presented absorbed boundaries based on complex mathematic model. Lee and Tassoulas in 2011 [44] implemented the mentioned boundaries into soil-structure interaction issues and observed a satisfactory performance. But still as with the completely adjusted layer, the complexity of use is one of the main drawbacks of this approach.

## 1.2 The design strain

The amount of axial strain has been investigated in various researches [25]to [48]. Diverse equations have been proposed for the amount of strain. Power et al. [45] have proposed Eq. (3);

$$\varepsilon_\alpha = \frac{V_{RP}}{C_p} \quad (3)$$

In which  $V_{RP}$  the maximum speed of land movement when P-wave emerges which equals to  $0.861 * V_{\max,v}$  and  $C_p$  equals to the maximum speed of P-wave movement in the soil and  $V_{\max,v}$  is the maximum speed of land movement in horizontal direction. When the impact angle is different, Eq. (4) can be used.

$$\varepsilon_\alpha = \frac{V_{RP}}{C_p} \cos^2 \varphi + r \frac{a_p}{C_p^2} \sin \varphi \cos^2 \varphi \quad (4)$$

$\varphi$  is the wave impact angle and  $a_p$  is the maximum velocity caused by land movement and  $r$  is the radius of the pipe or tunnel. Also, the amount of design strain equals to Eq. (5) according to the researches [46][47] in which  $V_{RS}$  and  $V_{RP}$  are the maximum speed of vertical shear wave SV equalling to  $1.0 * V_{\max,v}$  and the maximum speed of P-wave respectively and  $C_R$  equals to the maximum amount of the S-wave movement in the soil.

$$\varepsilon_\alpha = \frac{V_{RP}}{C_p} \quad OR \quad \varepsilon_\alpha = \frac{V_{RS}}{C_R} \quad (5)$$

According to the guideline ASCE-ALA 2005 [48], the seismic design of the buried pipelines is based on the maximum amount of the axial strain and approximate amounts are calculated based on the Eq. (6) in which  $V_g$  is to the maximum speed of land movement equaling to  $V_{\max,v}$  and  $C_a$  equals to 2000 meters per second irrespective of the type of soil and is employed as the wave propagation speed in the soil [25].

$$\varepsilon_\alpha = \frac{V_g}{\alpha \times C_a} \quad (6)$$

Also the parameter is used for RL waves and pressure P-waves equaling 1 and S-waves equal to 2. As a result, the maximum amounts of strains based on  $V_g$  produced by various ranges of earthquakes as is shown in Table 1. Gas and oil pipelines go through areas with diverse soils, considering the long length of pipelines. Furthermore, all the analyses were carried out in four types of soil given the fact that in most guidelines, including uniform building code 94 (UBC94) soils are classified into four groups [53]. It should be mentioned that equations (1~4) are based on the impact angle which leads to the maximum axial-pressure force. Fig. 1 Demonstrates the way a wave impacts the pipe and its angles with the pipe. D is the domain of wave propagation. Also the figure shows the amounts of sinusoidal wave which are consisted of the wave parallel to the pipe and the wave vertically parallel to the pipe [47]. It should also be mentioned that the amounts given in the equations in Table 1 are based on normalized earthquake spectra. In all cases, the amounts of axial strains calculated by ALA are less than the other equations (since the wave propagation speed is supposed to be 2000 m/s).

Based on laboratory reports presented by Newmark et al. the first sign of local buckling is shown in the Eq. (7) in which R is the pipe radius and t is the wall thickness of the pipe [49][50].

$$0.15 \frac{t}{R} < \varepsilon < 0.2 \frac{t}{R} \quad (7)$$

Based on researches done by Hosseini and Roudsari [51], a new equation was introduced to investigate the first point of local buckling for sandy soil (Eq. 8 and 9). Equation (8) depicts dense sandy soil and equation (9) depicts non-dense sandy soil [51].

$$0.17 \frac{t}{R^{1.5}} < \varepsilon < 0.26 \frac{t}{R^{1.5}} \quad (8)$$

$$0.15 \frac{t}{R^{1.1}} < \varepsilon < 0.34 \frac{t}{R^{1.1}} \quad (9)$$

**Table 2** The amounts of the maximum longitudinal strain permitted in design for different waves.

	SOIL TYPE	Loma Prieta	kobe	Imperial Valley	Northridge	Manjil
$V_g$		1.21	0.8	1.00	0.92	0.34
$\varepsilon_a \times 10^{-3}$ (ASCE-ALA)	I-IV	0.06	0.40	0.50	0.46	0.17
$\varepsilon_a \times 10^{-3}$ (HASHASH)	I	1.20	0.80	1.00	0.90	0.34
$\varepsilon_a \times 10^{-3}$ (HASHASH)	II	1.50	1.00	1.25	1.15	0.42
$\varepsilon_a \times 10^{-3}$ (HASHASH)	III	2.70	1.80	2.20	2.00	0.76
$\varepsilon_a \times 10^{-3}$ (HASHASH)	IV	4.90	3.20	4.00	3.70	1.40

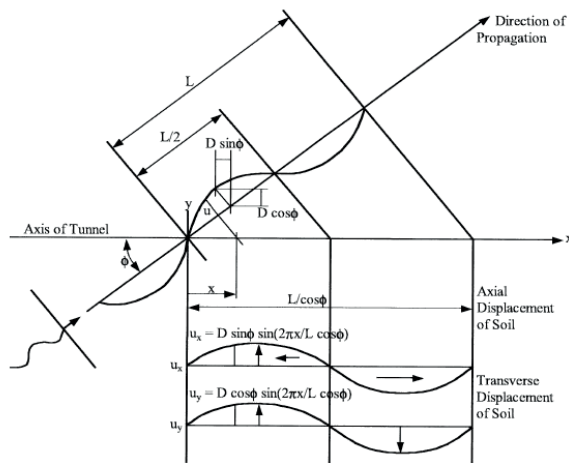


**Fig. 1** Waves propagate method and impact with the pipe and the way a longitudinal wave expands in the pipe [2].

Regarding the pipe diameter equaling to 1 meter and its thickness equaling to 1 centimeter, the minimum amounts of the strain to control local buckling is 0.003. Since the aim of this research is to investigate the effect of P-wave propagation on the seismic behaviour of steel pipelines, we embarked on investigating impact wave with the impact angle of zero degree.

## 2 Numerical modelling

The types of analyses employed were based on time history analyses and the wave propagation method in pipes and soil has been investigated. To carry out three-dimensional modelling, 1000 meters of pipeline were used to increase the precision of the analyses. The modelling was based on Beam theory on an elastic bed. To investigate the effect of changes in wave propagation speed without changing the frequency content of the wave, first sinusoidal wave with the same content together with changes in the speed of wave transmission was investigated. Then, five spectra of earthquakes were used to consider the effect of changes in various frequency contents on seismic behaviour of pipelines. The aim is to calculate the effect of wave propagation on the amounts of longitudinal strains affected by P-wave. The load is imposed in a way that the effect of P-wave on the pipe is calculated. First, all spectra were equaled to the acceleration basis of 1G in order to just investigate the effect of changes in frequency content. Then the scaled spectra were used by MATLAB according to boundary conditions and the meshing method. The boundary condition was introduced for each pipe element and the amounts of changes in place changed depending on the pipe length. During solution trend, all the amounts belonging to the imposed change in place in all soil types were considered. ABAQUS software was employed to do modelling [[52].

**Table 3** The properties of used sandy soil.

SAND TYPE	$\phi$	$\gamma \left( \frac{KN}{m^3} \right)$	$K$	$K_0$	$T_s$	$V_s \left( \frac{m}{s} \right)$	$V_p \left( \frac{m}{s} \right)$	$\lambda(m)$
I	35	21	0.7	1.5	0.4	625	1000	250
II	33	20	0.65	1.2	0.5	500	800	250
III	31	19	0.55	0.8	0.7	275	450	192.5
IV	30	18	0.50	0.5	1.0	150	250	150

**Table 4** The properties of used clayey soil.

CLAY TYPE	$\gamma \left( \frac{KN}{m^3} \right)$	$S_u \left( \frac{N}{m^2} \right)$	$T_s$	$V_s \left( \frac{m}{s} \right)$	$V_p \left( \frac{m}{s} \right)$	$\lambda(m)$
I	21	1.5	0.4	625	1000	250
II	20	1.2	0.5	500	800	250
III	19	0.8	0.7	275	450	192.5
IV	19	0.5	1.0	150	250	150

## 2.1 Pipe-soil interaction

There are various methods to model the soil. One of the acceptable methods in most worldwide guidelines is soil-spring equalization. In this method three springs with stiffness in three main directions were employed. The amounts of spring stiffness as well as their movement have been calculated by ASCE-ALA guideline [48]. In this research the soil-spring equalization method has been used. Non-linear springs have been employed to take soil-structure interaction into account (Fig. 2&3).

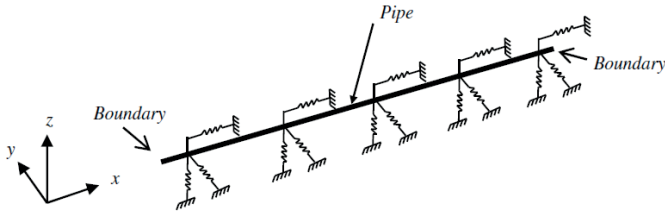


Fig. 2 Modelling of pipelines together with spring in different directions.

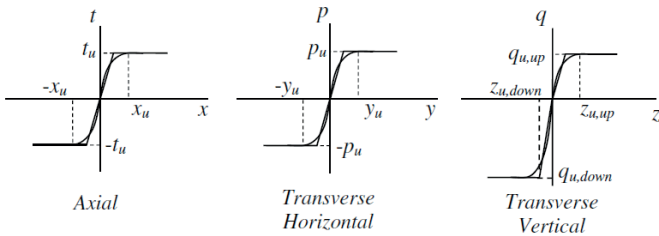


Fig. 3 The characteristics of modelled springs in three different directions of axial, transverse horizontal and transverse vertical.

To model the soil, two types of soil were employed; i.e. clayey and sandy soil, and each type of soil was classified into four groups based on the density and the wave propagation speed. Properties of the soil used in analyses can be seen in Tables (2, 3)[20][46], and[48]. In Table 3, the properties of sandy soil and in Table 4, the properties of clay soil can be observed. In this Table,  $\phi$  is sand internal friction coefficient,  $k$  is friction reduction coefficient between pipe and soil,  $K_0$  lateral resistance coefficient,  $S_u$  is undrained shear resistance of confined soil per N/m<sup>2</sup>,  $T$  is soil dynamic period per second,  $V_s$  is the shear wave speed in soil per m/s and  $\lambda$  is the wave length per meter[51].

## 2.2 Pipeline modelling and specifications

The pipe used in this research is made of steel X60 range which is one of the most common gas and oil transmission pipelines in the world. Ramberg-Osgood equation was employed to achieve the amounts of strain [50]; in which in terms of X60 pipe, the amounts of  $n$ ,  $r$ ,  $\sigma$  are 10, 12,  $413 \times 10^6$  N/m<sup>2</sup> respectively [50].

$$\varepsilon = \frac{\sigma}{E} \left[ 1 + \frac{n}{1+r} \left( \frac{\sigma}{\sigma_y} \right)^r \right] \quad (10)$$

## 2.3 Minimum Required Length of the Pipe Segment for Modelling

The length of the pipe used in the modelling should be in a way that the upper boundary condition does not affect the amounts of strain or the tension in middle element of the pipe. According to the researches [51], it became obvious that the minimum length of the required pipe in cohesive soil should equal to  $2\lambda$  and in granular soil should equal to  $4\lambda$  [51]. Pipeline of 1000 meters' length was used for both types of soil, regarding the fact that the maximum amounts of wave length equaled to 250 meters. Since modelling with pipe limited components of 1000 meters long with shell elements and three-dimensional soil model is really time-consuming, PIPE elements were employed to model the pipe which is a kind of beam element. Therefore, the only way to control local buckling in a pipe is to control the maximum amounts of strains.

It is possible to investigate the effect of pipe length while taking modal analysis of pipelines in soil into account in order to calculate the minimum required length of the pipeline. The effect of pipeline length on higher modes was investigated by Hosseini et al. [51]. It became obvious that if the length of pipe is considered infinite, the amounts of the limit state of angular frequency are obtained using Eq. (11).

$$\lim_{l \rightarrow \infty} \bar{\omega}_i = \sqrt{\frac{k_u}{m}} \quad (11)$$

It also became evident that if the length of pipe is not infinite, the amounts of  $\bar{\omega}_i$  contain the percentage difference equaling  $\beta$  [51].

$$\bar{\omega}_i = (1 + \beta) \sqrt{\frac{k_u}{m}} \quad (12)$$

$$\beta = \frac{m}{2k_u} \omega_i^2$$

In case the length of the pipe tends to the infinite,  $\beta$  tends to become zero. Otherwise, Eq. (13) is used to obtain the minimum required length of the pipe in order to obtain  $\beta$  acceptable percentage error [51].

$$l = \sqrt[4]{\frac{EI\alpha_i^2}{2\beta K_u}} \quad (13)$$

Hosseini et al. proposed equations for the minimum length of pipeline in sandy and clay soils using ASCE as well as Eq. (13) [Eq. 14 and 15] in which  $H$  is the depth of burial,  $N_{qh}$  is dimensionless coefficient and  $\zeta$  is dimensionless coefficient which is about 0.02 for dense sand and about 0.1 for loose sand and is approximately 0.3 for stiff clay and is about 0.05 for loose clay.

$$l = \sqrt[4]{\frac{\pi\alpha_i^2\zeta}{8\beta} \frac{Et}{\gamma} \frac{R^2}{N_{qh}} \left( 1 + \frac{R}{H} \right)} \quad (14)$$

$$l = \sqrt[4]{\frac{\pi\alpha_i^2\zeta}{8\beta} \frac{Et}{S_u} \frac{R^2}{N_{ch}} (H + R)} \quad (15)$$

## 2.4 The verification of modelling

Two different methods were used for model verification. In the first method to model one of the most respected papers in the field of wave propagation frequency values obtained are discussed and compared [51].

In the second method, the effect of two-dimensional modeling and comparison with conventional spring soil pipe and pipe have been investigated.

First, The amounts of frequency belonging to this research's model were compared with those of Hosseini et al. [51] so as to verify the modelling results. When it comes to models belonging to Hosseini et al. [51], the results of modal analysis of the first hundred modes were obtained and its diagram for clay soil (type 1) as well as the results of modal analysis in terms of samples used in this research can be observed in Fig. 4. Three models with the length of 200, 400 and 1000 meters were created to carry out verification and the amounts of frequency were obtained while taking 100 modes into consideration. It became obvious that in sample with the pipe length of 200 meters, the results depict the percentage difference of 7.9 and when it comes to samples with the pipe length of 400 meters, this difference reached to 5.86 % and when it comes to sample with the pipe length of 1000 meters, this difference comes to 2.22%. As it can be observed, when it comes to long pipes, the amount of difference is of little and can be overlooked. That's why pipes with the length of 1000 meters are employed in analyses.

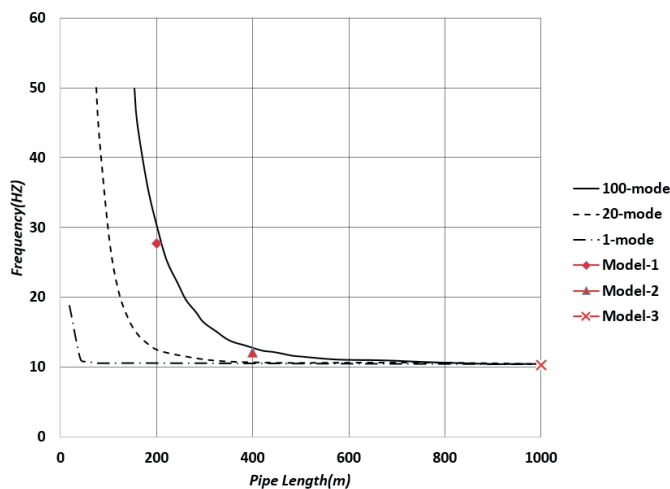


Fig. 4 Depicts the comparison between the obtained results of verification and the modelling belonging to Hosseini et al.[51]

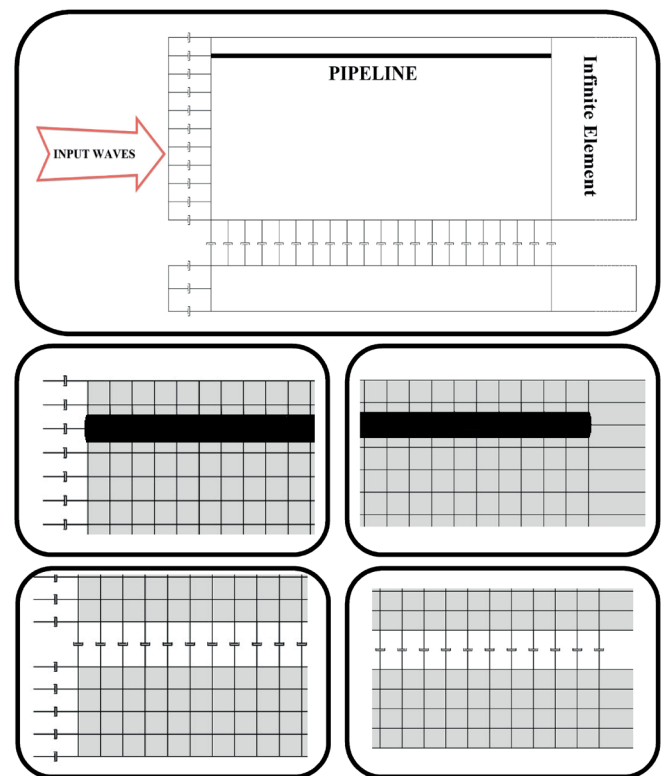


Fig. 5 The model configuration in 2D analyses with ABAQUS.

Second, to do more comparison, the analysis of two dimensional modelling by CPE4R elements was employed to model the wave propagation. For example, one of the analyses with soil type of IV was analysed under the sinusoidal wave. Fig. 5 shows the way of modelling and meshing. The length of the pipe used in this model is the same as the previous models, equalling to 1000 meters. Also, the soil depth of 150 meters is employed to increase the accuracy of modelling. Infinite elements in boundary points were used to prevent the reflection of waves. The amounts of input stimulation were done through one side and the wave created by soil stiffness moves from the left to the right at an appropriate speed. Due to the existence of absorbed boundary, the propagated wave has an insignificant reflecting part. However, it does not have a big impact on the results because of considering the long length of the pipe. Elements one tenth (1/10) of wave length were employed to prevent the break of the wave and meshing was conducted using  $1 \times 1\text{m}$  elements. The number of elements used for modelling soil was 150,000. The time of analysis was extremely long because of using two-dimensional elements. According to this analysis, it became clear that the results derived from pipe and spring analysis correspond with those of two dimensional samples.

Fig. 6 depicts the way the amounts of stress expand in the soil. It became obvious that the amounts of propagational wave are spread and distributed in the soil properly and that the amounts of return wave are insignificant. Also, the ratio of the domain of the imposed wave to that of the return wave is 0.012. Given the long length of the pipe, the length of 100 meters was employed to investigate the results. Furthermore, the chosen

area is located in the middle of the pipeline in order to reduce the effect of the boundary condition on the results. Fig. 7 shows the comparison of the amounts of strain in the pipeline in both models. It became evident that the amounts of Maximum tension strain produced in the pipe in both samples have the maximum difference, equaling 3.4 per cent.

The amounts of compressive strain obtained from 2D analyses had a less than 10.4% difference from those obtained from samples modelled by PIPE and PSI element.

### 3 The analyses cases

To investigate the effect of wave propagation speed as well as the impact of soil type various analysis was performed.

First, because of time-consuming analyzes the impact of the sinusoidal wave is discussed. The analysis was performed in different soils and with different wave propagation speed. After that time history analysis was performed for different soils and under five earthquake spectra.

#### 3.1 Pulse wave propagation

First the effect of wave propagational speed on sinusoidal wave was investigated. As can be seen in Table 4, the amounts of axial strain in pipe's middle elements in four different types of soil and in various frequencies were investigated. Also, the wave propagational speed in each type of soil was modeled with respect to the P-wave propagation speed in soil.

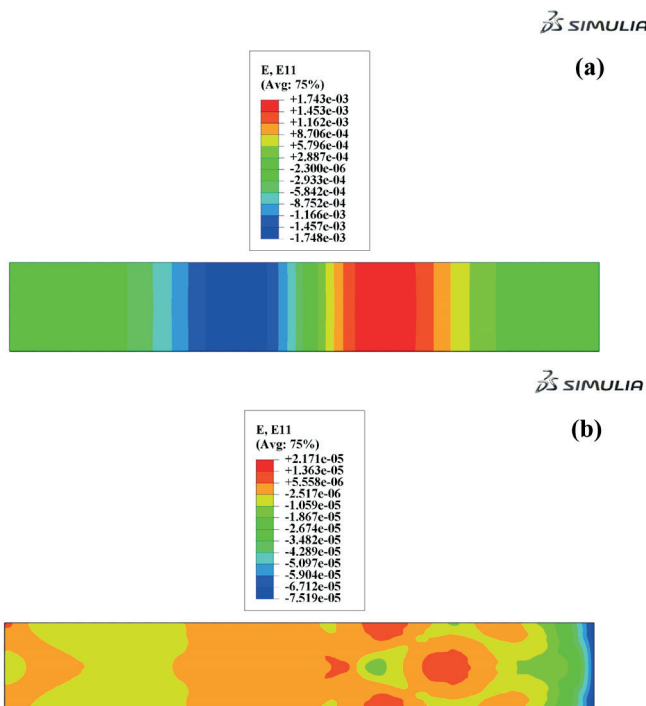
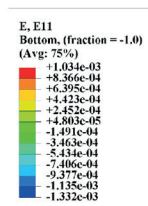
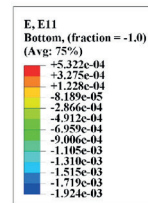
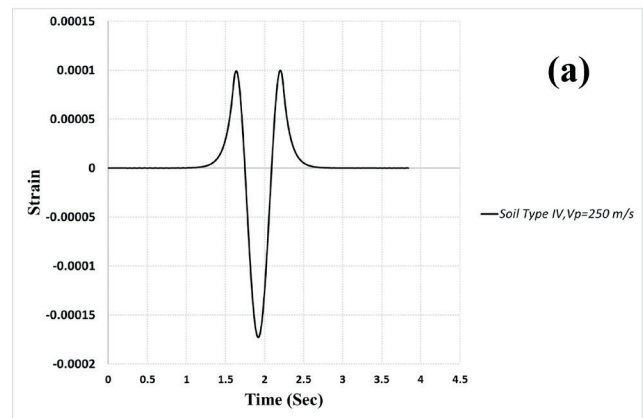


Fig. 6 The contour of wave propagation in 2D analyses in soils. (a) The propagating waves. (b) The reflecting wave.

Fig. 7 The comparison between the result of (a) PSI and spring model, (b) maximum compressive strain, (c) maximum tension strain in 2D analyses.

In this modelling, one type of sinusoidal wave with an equaled acceleration of 1G was used and the only difference between analyses is the different amounts of vibration frequency belonging to each wave. For instance, Fig. 8 shows one of the diagrams obtained for the strain in four different types of soil with the frequency of 1.56 hertz. It became clear that the maximum amount of strain belongs to soils with low velocity of wave propagation, equaling to 0.0017. Furthermore, the amounts of phase difference created by the velocity of wave move in soil around the pipe were calculated, equaling to 0.52.

Considering Table 5, it became clear that the amounts of strain in stiff soils (types I and II) are less than those of looser soils and as the wave propagation speed increases, the amounts of strain decrease. Furthermore, the effect of wave frequency content on the wave propagation speed should not be underestimated. Waves with different frequency contents had various effects on the amounts of strain.

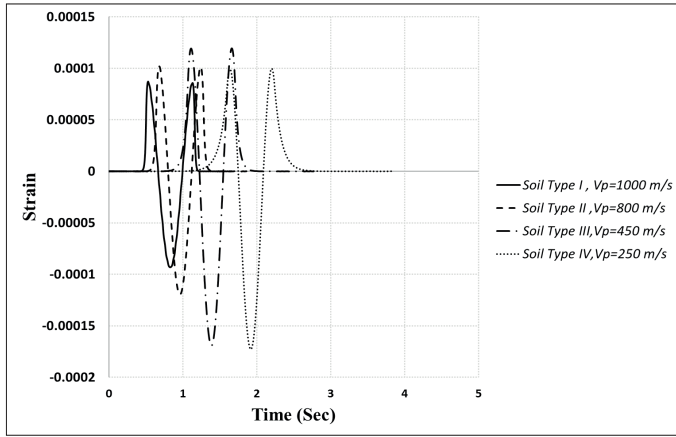


Fig. 8 The amount of strain in sinusoidal wave with frequency of 1.56 Hz.

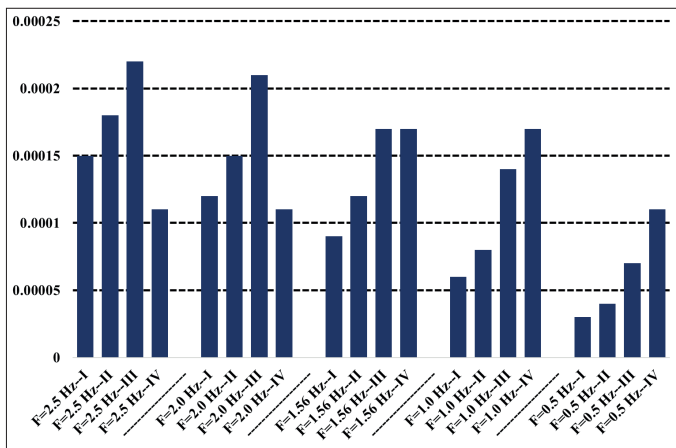


Fig. 9 The amount of maximum strain in sinusoidal wave with all five frequencies.

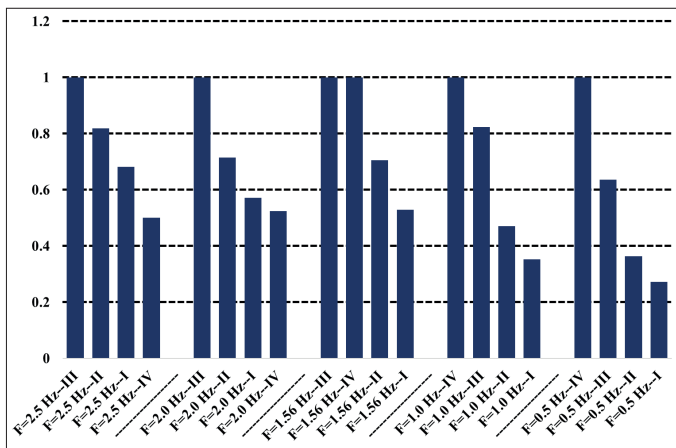


Fig. 10 The relative amounts of strain in different frequencies. Horizontal axis indicates soil types and vertical axis indicates the ratio of strain to the maximum strain.

As the amount of vibration frequency decreases, the amounts of strain in low speeds will be in a crisis and as the amount of frequency increases, the most amount of strain happens in terms of wave propagation speed of 450 m/s instead of 250 m/s. The amounts of strains in each frequency can be observed in Fig. 9. To investigate more, the amounts of strains in four samples were equaled with respect to the maximum amount of strain and equaled trends for the five different frequencies can be seen in Fig. 10.

With respect to Fig. 10, it can be seen that the maximum amounts of strain are produced in the wave speed of 450 m/s and soil type III in terms of 2 and 2.5 Hz frequencies and in other samples with 1.56, 1.0, 0.5 Hz frequencies the most amounts of strain are found in soil type IV. As a result, it can be concluded that wave propagation speed has a significant effect on the amounts of responses and in soil types of III and IV (in which the wave motion speed is less), the amounts of strain are more than those of soil types I and II. In other words, the stiffer the soil is, the less the amounts of strain are. Also, it became obvious that as the frequency of imposed wave increases, the amounts of axial strain increases simultaneously. For instance, in soil type I, the change in wave frequency from 2.5 Hz to 0.5 Hz will lead to strains ranging from 0.00015 to 0.0003 which indicates the amount of reduction in strain equals to %20.

### 3.2 Time history response

To investigate the effect of different vibration frequencies of spectra with different frequency contents are used. The analysis was performed in different soils and with different wave propagation speed. After that time history analysis was performed for different soils and under five earthquake spectra. Then, the research embarks on investigating the effect of wave propagation speed after using five earthquake spectra on the pipelines. Figures 11 to 16 indicate the amounts of strain for three types of time history analyses.

Table 5 The amounts of axial strain obtained for the middle elements under the influence of sinusoidal wave with different frequencies.

Soil Type	$V_p (m/s)$	$V_{particle} (m/s)$	Frequency	$\epsilon_a$
I	1000	0.62	2.5	0.00015
II	800	0.62	2.5	0.00018
III	450	0.62	2.5	0.00022
IV	250	0.62	2.5	0.00011
I	1000	0.78	2	0.00012
II	800	0.78	2	0.00015
III	450	0.78	2	0.00021
IV	250	0.78	2	0.00011
I	1000	1.00	1.56	0.00009
II	800	1.00	1.56	0.00012
III	450	1.00	1.56	0.00017
IV	250	1.00	1.56	0.00017
I	1000	1.56	1	0.00006
II	800	1.56	1	0.00008
III	450	1.56	1	0.00014
IV	250	1.56	1	0.00017
I	1000	3.12	0.5	0.00003
II	800	3.12	0.5	0.00004
III	450	3.12	0.5	0.00007
IV	250	3.12	0.5	0.00011



In Fig. 11 and Fig.12, the diagram is shown for Manjil earthquake's spectrum and for sandy and clayey soils respectively. The comparison of strain amounts for Manjil spectrum is of importance because this spectrum has the minimum amount of velocity ( $V_g$ ) among existing accelerograms. It also became evident that the maximum amount of strain in both types of sandy and clayey soil occurs in soil type IV. The velocity of longitudinal wave propagation of this soil type reaches 250 meters per second. Fig. 13 and Fig. 14 indicate the strain diagram belonging to Imperial Valley earthquake's spectrum for two types of sandy and clayey soils respectively. The reason behind studying this accelerogram is evaluating the effect of frequency content on the amounts of analysis. It became evident that the maximum amounts of strain have been created in soil type III that velocity of longitudinal wave propagation equals to 450 meters per second. The most striking point in this figure is the change in the location of the maximum strain created in various soil types together with the different velocities of wave propagation, in a way that the increase in the velocity of wave propagation has led to the formation of new peaks along the diagram, resulting in the relocation of the maximum amounts of strain during the time. For instance, with regard to sandy soil, when the velocity of wave propagation reaches to 250 meters per second, it is possible to observe three peaks with the approximate strain of 0.00145, whereas when the velocity of wave propagation increases, the effect of frequency content is more noticeable and there is a decrease in the number of peak points in the diagram. Furthermore, Fig. 15 and Fig. 16 indicate the results

for Northridge earthquake's spectrum. This accelerogram has the shortest analysis time among the chosen accelerograms. Although this accelerogram recorded the shortest time, the procedure of the previous accelerograms was also repeated in this accelerogram. In this analysis, the highest amount of strain was created in soil type IV which has less stiffness. It also became evident that the amounts of strain in clayey soil are more than those of sandy soil. What's more, the change in soil type leads to a change in responses as well as the behavior of pipeline. For instance, the time for creating the maximum response in every spectrum is different in the two types of soils. Also, the effect of soil material on responses is evident.

The end results can be observed in Table 6 in order to compare the maximum and minimum amounts of axial strain in the pipe middle element as well as the absolute value of the maximum and minimum interval between amounts of strain for each spectrum and both soil types.

It was observed that although all earthquake records had the same acceleration, i.e. 1G, in Loma-Prieta record (in which the maximum wave speed exceeded the other ones and the wave speed equaled to 1.21 m/s) the amounts of strained produced exceeded the other records and equaled to 0.0028 and that Manjil record with the maximum speed of 0.34 m/s (while having the minimum speed among the records) had the minimum amount of axial strain, equaling to 0.00028. This indicates the enormous effect of frequency content on the amounts of response so much so that the maximum amount of strain is ten times more than its minimum amount.

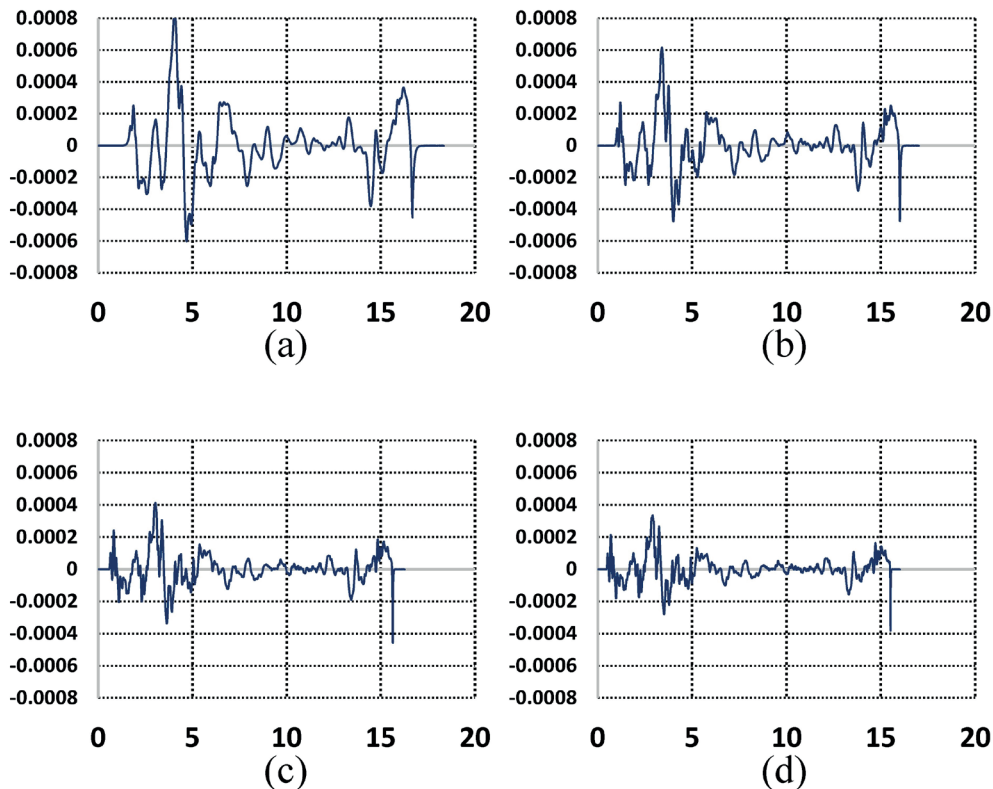


Fig. 11 The amounts of strain in Manjil earthquake for the speeds of 250 m/s, 450 m/s, 800 m/s and 1000 m/s in sandy soil.

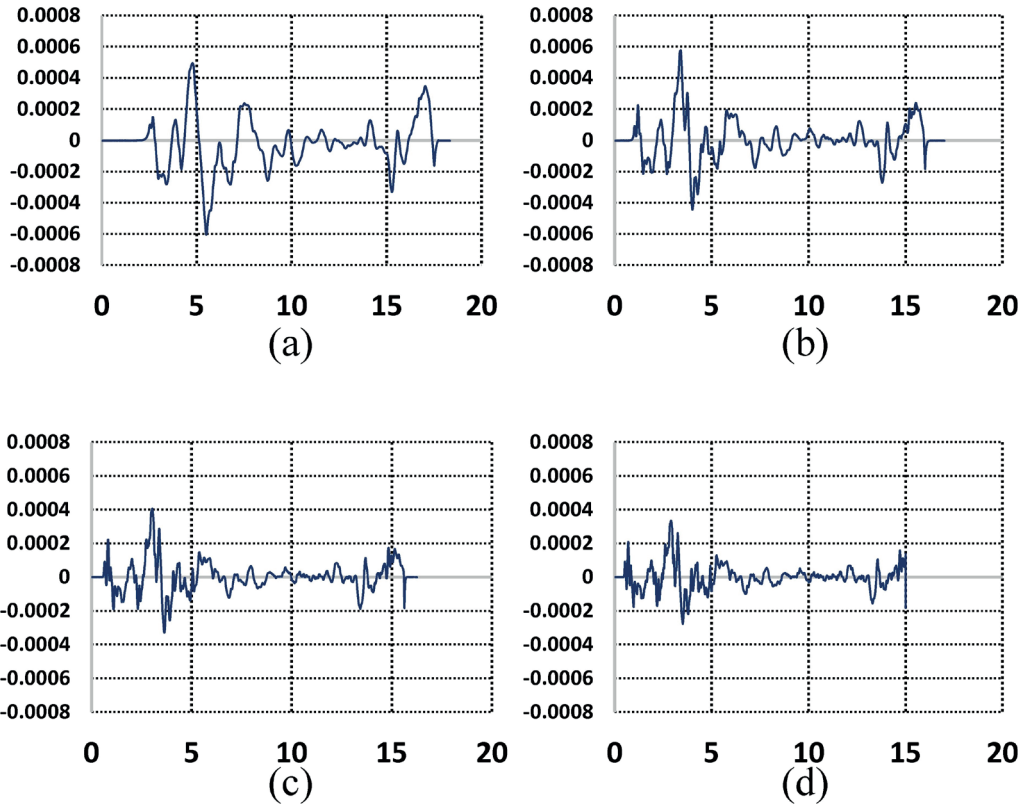


Fig. 12 The amounts of strain in Manjil earthquake for the speeds of 250 m/s, 450 m/s, 800 m/s and 1000 m/s in clayey soil.

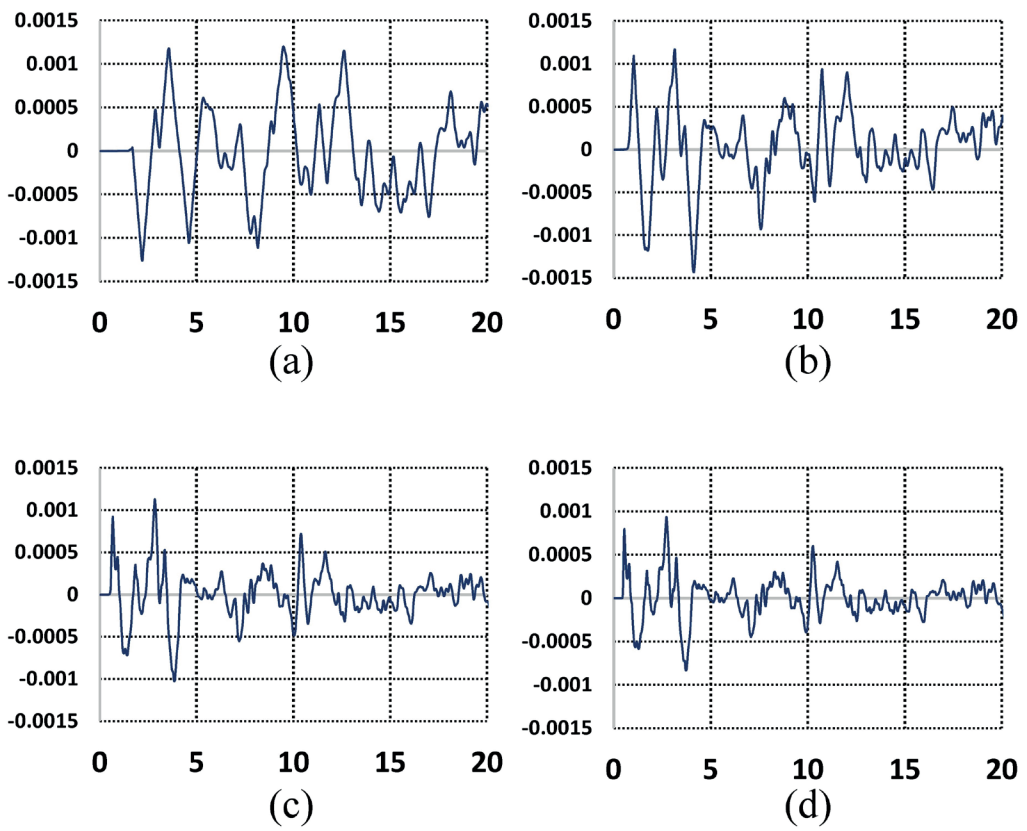


Fig. 13 The amounts of strain in Imperial Valley earthquake for the speeds of 250 m/s, 450 m/s, 800 m/s and 1000 m/s in sandy soil.

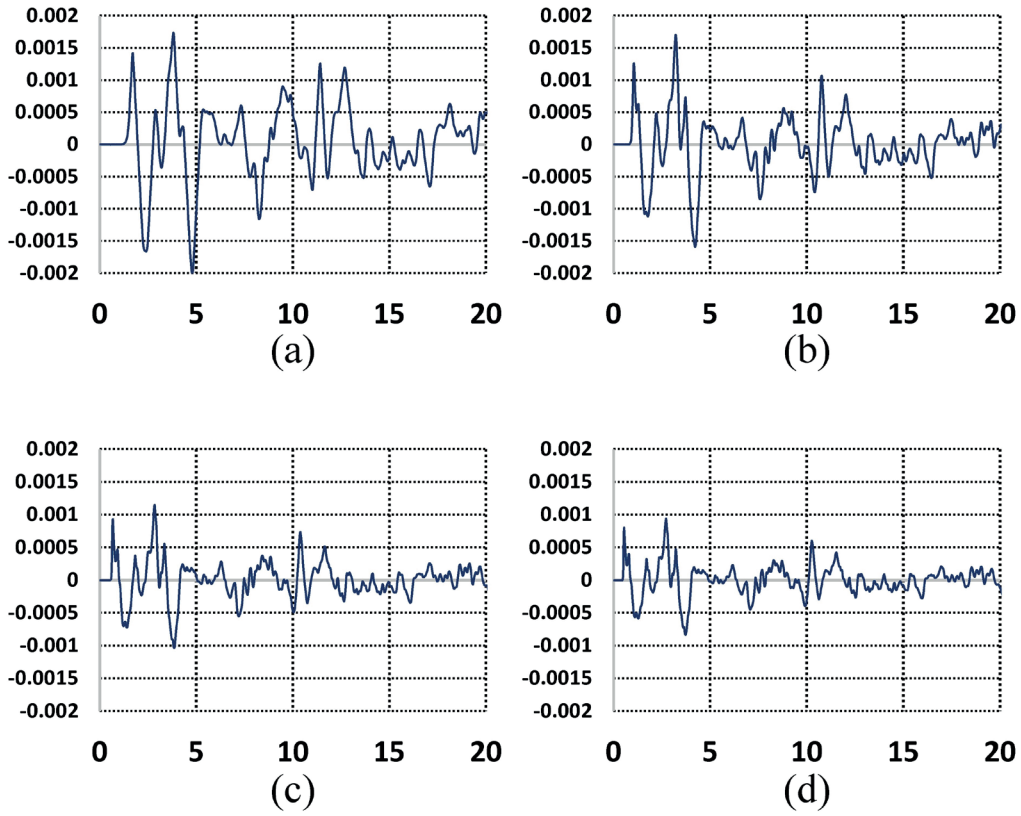


Fig. 14 The amounts of strain in Imperial Valley earthquake for the speeds of 250 m/s, 450 m/s, 800 m/s and 1000 m/s in clayey soil.

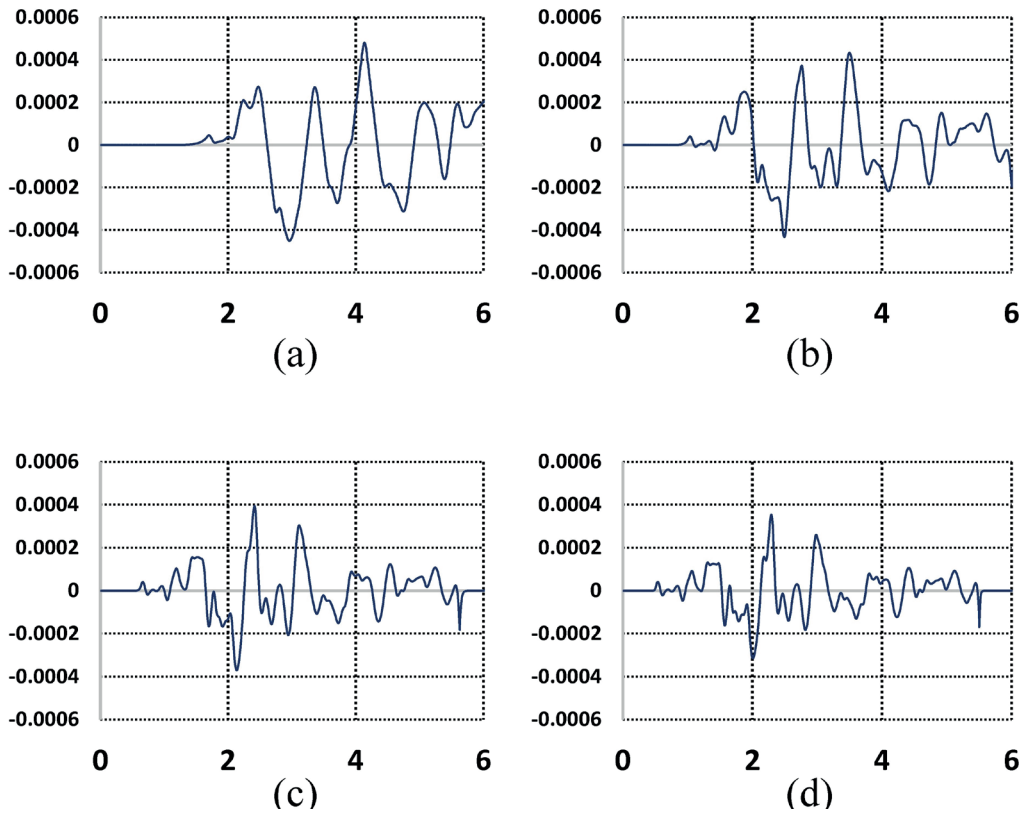


Fig. 15 The amounts of strain in Northridge earthquake for the speeds of 250 m/s, 450 m/s, 800 m/s and 1000 m/s in sandy soil.

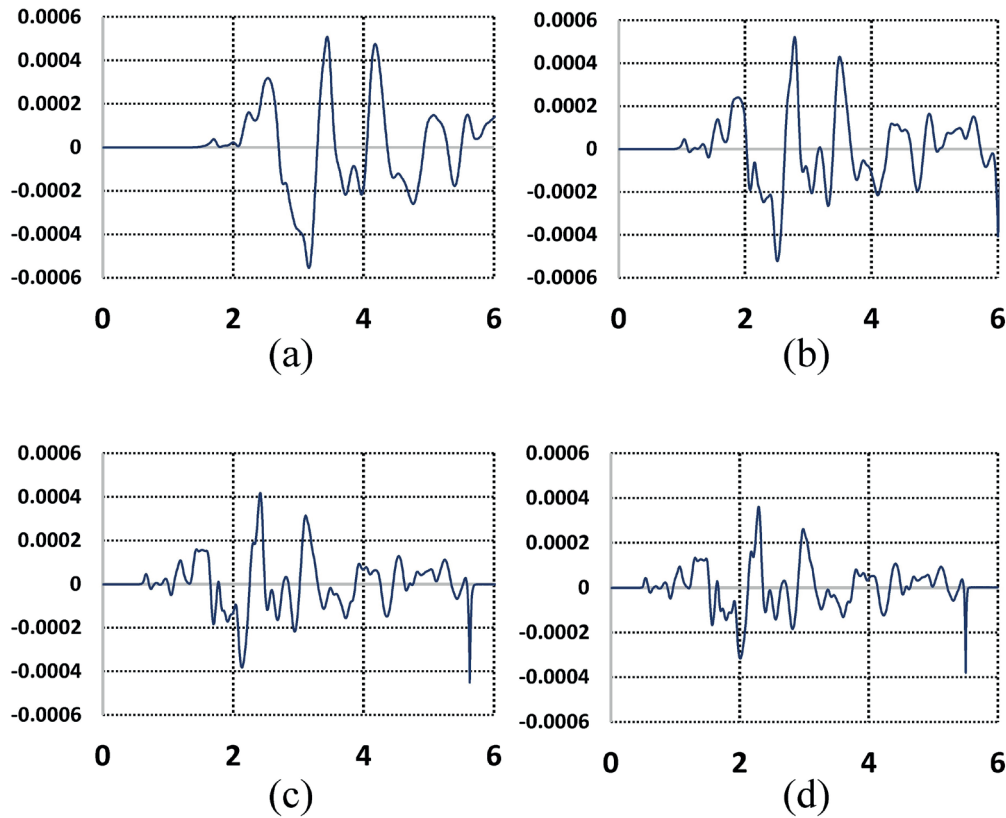


Fig. 16 The amounts of strain in Northridge earthquake for the speeds of 250 m/s, 450 m/s, 800 m/s and 1000 m/s in clayey soil.

Also after investigating the amounts of strain in both soil types of clay and sandy under a particular record, it became obvious that the amounts of strain in clayey soil are more than those in sandy soil.

For example, in Loma-Prieta earthquake the ratio of strain produced in sandy soil to clayey soil in soil type II is 0.625. Furthermore, for Kobe, Imperial Valley, Northridge as well as Manjil spectra were 0.627, 0.987, 0.829 and 0.92 respectively. The ratio of minimum to maximum strain values in the clayey soils in different soil type (type I to type IV) in Loma-Prieta, Kobe, Imperial Valley, Northridge, and Manjil spectra were equal to 0.55 and 0.42 and 0.57 0.81 0.63 respectively. In sandy soil were equal to 0.63, 0.67, 0.58, 0.79, and 0.47 respectively. The average of the values of the reduced strain in different type of soil could reduce the amount of strain to be considered equal to 0.592 for clay soils, and equal to 0.61 for sandy soil.

To investigate the effect of wave propagation speed on the amounts of strain more precisely, Table 6 was equaled based on the maximum amount of strain. It shows the ratio of strains to the P-wave propagation speed in both soil types of sandy and clay. In both sample types of soil, the maximum strain is observed in soil types III and IV (which their longitudinal wave propagation speed equals to 250 m/s and 450 m/s). Also, the minimum amounts of strain belonged to soil type I with wave propagation speed of 1000 m/s.

Table 6 The characteristics of the maximum amounts of strain obtained for soils in different spectra.

Name	Soil Type	$V_p \left( \frac{m}{s} \right)$	$\varepsilon_a - \text{sandy oil}$	$\varepsilon_a - \text{clayey oil}$
Loma Prieta	IV	250	0.00137	0.00200
	III	450	0.00200	0.00280
	II	800	0.00197	0.00275
	I	1000	0.00126	0.00176
kobe	IV	250	0.00088	0.00160
	III	450	0.00121	0.00193
	II	800	0.00100	0.00101
	I	1000	0.00081	0.00082
Imperial Valley	IV	250	0.00084	0.00133
	III	450	0.00143	0.00145
	II	800	0.00103	0.00103
	I	1000	0.00083	0.00083
Northridge	IV	250	0.00032	0.00040
	III	450	0.00039	0.00047
	II	800	0.00037	0.00045
	I	1000	0.00031	0.00038
Manjil	IV	250	0.00060	0.00060
	III	450	0.00044	0.00048
	II	800	0.00033	0.00046
	I	1000	0.00028	0.00038

Based on the conducted Time History analyses, it can be observed that a change in the velocity of wave propagation in every record can lead to a change in the amounts of strains and the time of their occurrence, so much so that a change in velocity can result in the increase or decrease in the peaks of maximum strain along the recording time of an earthquake.

It also became obvious that the amounts of strain in clay soil are more than those in sandy soil. On average, the ratio of strain in sandy soil to clay soil is 0.81 for all samples. The most effect can be seen in loose soil, equaling 0.733. When it comes to hard soil, the difference between the amounts of strain is less, equaling to 0.846.

#### 4 Conclusions

Two type of analyses used in this paper. First, because of time-consuming analyzes the impact of the sinusoidal wave is discussed. The analysis was performed in different soils and with different wave propagation speed.

After that time history analysis was performed for different soils and under five earthquake spectra.

According to research, the following results were obtained.

- Modeled by beam elements and PSI element has good accuracy in comparison with two-dimensional modeling of soil. It became evident that the amounts of Maximum tension strain produced in the pipe have the maximum difference, equaling 3.4 per cent. The result is avoiding time consuming 2D analyses, and use PIPE and Psi element, and saving the time.
- According to sinusoidal p-wave, it was clear that as the frequency of imposed wave increases, the amounts of axial strain increases simultaneously. For instance, in soil type I, the change in wave frequency from 2.5 Hz to 0.5 Hz will lead to strains ranging from 0.00015 to 0.0003 which indicates the amount of reduction in strain equals to %20.
- According to time history analyses it was obvious that the amounts of strain in clayey soil are more than those of sandy soil. What's more, the change in soil type leads to a change in responses as well as the behavior of pipeline. For instance, the time for creating the maximum response in every spectrum is different in the two types of soils. Also, the effect of soil material on responses is evident.
- It also became evident that the effect of the velocity of the earth movement (Manjil earthquake being the least, equaling to 0.34 meters per second, and Loma-Prieta being the most, equaling to 1.21 meters per second) on the amounts of strain is very high. Considering the same amounts of acceleration, the ratio of the maximum strain in Manjil to Loma Prieta equal to 10 percent.
- The amounts of strain in clay soil are more than those in sandy soil. On average, the ratio of strain in sandy soil to clay soil is 0.81 for all samples. The most effect can be seen in loose soil, equaling 0.733. When it comes to hard soil, the difference between the amounts of strain is less, equaling to 0.846.

#### References

- [1] Kennedy, R. P., Chow, A. M., Williamson, A. M. "Fault movement effects on buried oil pipeline.". *Transportation engineering journal of the American Society of Civil Engineers*, 103(5), pp. 617–633. 1977.
- [2] Choo, Y. W., Abdoun, T. H., O'Rourke, M. J., Ha, D. "Remediation for buried pipeline systems under permanent ground deformation.". *Soil Dynamics and Earthquake Engineering*, 27(12), pp. 1043–1055. 2007. <https://doi.org/10.1016/j.soildyn.2007.04.002>
- [3] Datta, T. K. "Seismic response of buried pipelines: a state-of-the-art review.". *Nuclear engineering and design*, 192(2), pp. 271–284. 1999. [https://doi.org/10.1016/S0029-5493\(99\)00113-2](https://doi.org/10.1016/S0029-5493(99)00113-2)
- [4] Moradi, M., Rojhani, M., Galandarzadeh, A., Takada, S. "Centrifuge modelling of buried continuous pipelines subjected to normal faulting.". *Earthquake Engineering and Engineering Vibration*, 12(1), pp. 155–164. 2013. <https://doi.org/10.1111/j.1548-1395.2010.01078.x>
- [5] Karamitros, D. K., Bouckovalas, G. D., Kouretzis, G. P. "Stress analysis of buried steel pipelines at strike-slip fault crossings.". *Soil Dynamics and Earthquake Engineering*, 27(3), pp. 200–211. 2007. <https://doi.org/10.1016/j.soildyn.2006.08.001>
- [6] Karamitros, D. K., Bouckovalas, G. D., Kouretzis, G. P., Gkesouli, V. "An analytical method for strength verification of buried steel pipelines at normal fault crossings.". *Soil Dynamics and Earthquake Engineering*, 31(11), pp. 1452–1464. 2011. <https://doi.org/10.1016/j.soildyn.2011.05.012>
- [7] Kouretzis, G. P., Andrianopoulos, K. I., Sloan, S. W., Carter, J. P. "Analysis of circular tunnels due to seismic P-wave propagation, with emphasis on unreinforced concrete liners.". *Computers and Geotechnics*, 55, pp. 187–194. 2014. <https://doi.org/10.1016/j.compgeo.2013.08.012>
- [8] Kouretzis, G. P., Sloan, S. W., Carter, J. P. "Effect of interface friction on tunnel liner internal forces due to seismic S-and P-wave propagation.". *Soil Dynamics and Earthquake Engineering*, 46, pp. 41–51. 2013. <https://doi.org/10.1111/j.1548-1395.2010.01078.x>
- [9] Sedarat, H., Kozak, A., Hashash, Y. M. A., Shamsabadi, A., Krimotat, A. "Contact interface in seismic analysis of circular tunnels.". *Tunnelling and Underground Space Technology*, 24(4), pp. 482–490. 2009. <https://doi.org/10.1016/j.tust.2008.11.002>
- [10] Joshi, S., Prashant, A., Deb, A., Jain, S. K. "Analysis of buried pipelines subjected to reverse fault motion.". *Soil Dynamics and Earthquake Engineering*, 31(7), pp. 930–940. 2011. <https://doi.org/10.1016/j.soildyn.2011.02.003>
- [11] Baziar, M. H., Nabizadeh, A., Mehrabi, R., Lee, C. J., Hung, W. Y. "Evaluation of underground tunnel response to reverse fault rupture using numerical approach.". *Soil Dynamics and Earthquake Engineering*, 83, pp. 1–17. 2016. <https://doi.org/10.1016/j.soildyn.2015.11.005>
- [12] Jalali, H. H., Rofooei, F. R., Attari, N. K. A., Samadian, M. "Experimental and finite element study of the reverse faulting effects on buried continuous steel gas pipelines.". *Soil Dynamics and Earthquake Engineering*, 86, pp. 1–14. 2016. <https://doi.org/10.1016/j.soildyn.2016.04.006>
- [13] Karamitros, D. K., Bouckovalas, G. D., Kouretzis, G. P., Gkesouli, V. "An analytical method for strength verification of buried steel pipelines at normal fault crossings.". *Soil Dynamics and Earthquake Engineering*, 31(11), pp. 1452–1464. 2011. <https://doi.org/10.1016/j.soildyn.2011.05.012>
- [14] Saberi, M., Behnamfar, F., Vafaeian, M. "A semi-analytical model for estimating seismic behaviour of buried steel pipes at bend point under propagating waves.". *Bulletin of Earthquake Engineering*, 1(3), pp. : 1373–1402. 2013. <https://doi.org/10.1007/s10518-013-9430-y>
- [15] Saberi, M., Halabian, A. M., Vafaeian, M. "Numerical analysis of buried steel pipelines under earthquake excitations.". In: *Pan-Am CGS Geotechnical Conference*, 2011. <http://geoserver.ing.puc.cl/info/conferences/PanAm2011/panam2011/pdfs/GEO11Paper847.pdf>

- [16] Kourtezis, G. P., Bouckovalas, G. D., Karamitros, D. K. "Seismic verification of long cylindrical underground structures considering Rayleigh wave effects." *Tunnelling and Underground Space Technology*, 26(6), pp. 789–794. 2011. <https://doi.org/10.1016/j.tust.2011.05.001>
- [17] Kourtezis, G. P., Bouckovalas, G. D., Gantes, C. J. "Analytical calculation of blast-induced strains to buried pipelines." *International Journal of Impact Engineering*, 34(10), pp. 1683–1704. 2007. <https://doi.org/10.1016/j.ijimpeng.2006.08.008>
- [18] Ewing, W. M., Jardetzky, W. S., Press, F. "Elastic waves in layered media." *Physics Today*, 10(12), p. 27. 1957. <https://doi.org/10.1063/1.3060203>
- [19] Kuesel, Thumas R. "Earthquake design criteria for subways." *Journal of the structural division*, 95(6), pp. 1213–1231. 1969.
- [20] Leimbach, K. R., Sterkel, H. P. "Comparison of multiple support excitation solution techniques for piping systems." *Nuclear Engineering and Design*, 57(2), pp. 295–307. 1980. [https://doi.org/10.1016/0029-5493\(80\)90108-9](https://doi.org/10.1016/0029-5493(80)90108-9)
- [21] O'Rourke, M. J., El Hmadi, K. "Analysis of continuous buried pipelines for seismic wave effects." *Earthquake engineering & structural dynamics*, 16(6), pp. 917–929. 1988. <https://doi.org/10.1002/eqe.4290160611>
- [22] Ezzatyazdi, P., Jahankhah, H. "Practical suggestions for 2d finite element modelling of soil-structure interaction problems." In *Second European conference on earthquake engineering and seismology, Istanbul, Aug. 25–29, 2014*. [http://www.eaee.org/Media/Default/2ECCES/2ecces\\_eaee/1568.pdf](http://www.eaee.org/Media/Default/2ECCES/2ecces_eaee/1568.pdf)
- [23] Manolis, G. D., Tetepoulidis, P. I., Talaslidis, D. G., Apostolidis, G. "Seismic analysis of buried pipeline in a 3D soil continuum." *Engineering analysis with boundary element*, 15(4), pp. 371–394. 1995. [https://doi.org/10.1016/0955-7997\(95\)00035-M](https://doi.org/10.1016/0955-7997(95)00035-M)
- [24] Hosseini, M., Ajideh, H. "Seismic analysis of buried jointed pipes considering multi-node excitations and wave propagation phenomena." In: *Proceedings of the Pipelines 2001 Conference, ASCE, San Diego, USA. 2001*. [https://doi.org/10.1061/40574\(2001\)73](https://doi.org/10.1061/40574(2001)73)
- [25] Hosseini, M., MehrzadTahamouliRoudsari. "Minimum Effective Length and Modified Criteria for Damage Evaluation of Continuous Buried Straight Steel Pipelines Subjected to Seismic Waves." *Journal of Pipeline Systems Engineering and Practice*, 8(49), 04014018. 2015. [https://doi.org/10.1061/\(ASCE\)PS.1949-1204.0000193](https://doi.org/10.1061/(ASCE)PS.1949-1204.0000193)
- [26] Roudsari, M., Samet, S., Nuraie, N., Sohaei, S. "Numerically Based Analysis of Buried GRP Pipelines under Earthquake Wave Propagation and Landslide Effects." *Periodica Polytechnica Civil Engineering*, 61(2), pp. 292–299. 2017. <https://doi.org/10.3311/PPci.9339>
- [27] O'Rourke, M. J., and K. El-Hmadi. "Earthquake ground wave effects on buried piping." In *Proceedings of the 1985 Pressure Vessels and Piping Conference: Seismic Performance of Pipelines and Storage Tank. (Brown, S. J. (Ed.)), pp. 165–171. 1985*.
- [28] Kramer, S. L. "Geotechnical earthquake engineering." In *prentice-Hall international series in civil engineering and engineering mechanics. "Prentice-Hall, New Jersey. p. 653. 1996*.
- [29] Lysmer, John. "Finite dynamic model for infinite media." *Journal of the Engineering Mechanics Division*, 95(4), pp. 859–878. 1969.
- [30] Engquist, B., Majda, A. "Absorbing boundary conditions for numerical simulation of waves." *Proceedings of the National Academy of Sciences*, 74(5), pp. 1765–1766. 1977. <https://www.ncbi.nlm.nih.gov/pmc/articles/PMC430991/pdf/pnas00027-0007.pdf>
- [31] Ang A. S., Newmark, N. M. "Development of a Transmitting Boundary for Numerical Wave Motion Calculations." *Newmark (Nathan M) Consulting Engineering Services Urbana Ill, 1977*. <http://oai.dtic.mil/oai/oai?verb=getRecord&metadataPrefix=html&identifier=AD0722087>
- [32] Smith, W. D. "A nonreflecting plane boundary for wave propagation problems." *Journal of Computational Physics*, 15(4), pp. 492–503. 1974. [https://doi.org/10.1016/0021-9991\(74\)90075-8](https://doi.org/10.1016/0021-9991(74)90075-8)
- [33] Liao, Z. P., Wong, H. L. "A transmitting boundary for the numerical simulation of elastic wave propagation." *International Journal of Soil Dynamics and Earthquake Engineering*, 3(4), pp. 174–183. 1984. [https://doi.org/10.1016/0261-7277\(84\)90033-0](https://doi.org/10.1016/0261-7277(84)90033-0)
- [34] Kausel, Eduardo. "Local transmitting boundaries." *Journal of engineering mechanics*, 114(6), pp. 1011–1027. 1988. [http://dx.doi.org/10.1061/\(ASCE\)0733-9399\(1988\)114:6\(1011\)](http://dx.doi.org/10.1061/(ASCE)0733-9399(1988)114:6(1011))
- [35] Deeks, A. J., Randolph. M. F. "Axisymmetric time-domain transmitting boundaries." *Journal of Engineering Mechanics*, 120(1), pp. 25–42. 1994. [http://dx.doi.org/10.1061/\(ASCE\)0733-9399\(1994\)120:1\(25\)](http://dx.doi.org/10.1061/(ASCE)0733-9399(1994)120:1(25))
- [36] Liu, J., Gu, Y., Du, Y. "Consistent viscous-spring artificial boundaries and viscous-spring boundary elements." *Yantu Gongcheng Xuebao (Chinese Journal of Geotechnical Engineering)*, 28(9), pp. 1070–1075. 2006.
- [37] Du, X., Zhao. M. "A local time-domain transmitting boundary for simulating cylindrical elastic wave propagation in infinite media." *Soil Dynamics and Earthquake Engineering*, 30(9), pp. 937–946. 2010. <https://doi.org/10.1016/j.soildyn.2010.04.004>
- [38] Li, P., Er-xiang S. "A high-order time-domain transmitting boundary for cylindrical wave propagation problems in unbounded saturated poroelastic media." *Soil Dynamics and Earthquake Engineering*, 48, pp. 48–62. 2013. <https://doi.org/10.1016/j.soildyn.2013.01.006>
- [39] Berenger, J-P. "A perfectly matched layer for the absorption of electromagnetic waves." *Journal of computational physics*, 114(2), pp. 185–200. 1994. <https://doi.org/10.1006/jcph.1994.1159>
- [40] Basu, U. "Explicit finite element perfectly matched layer for transient three-dimensional elastic waves." *International Journal for Numerical Methods in Engineering*, 77(2), pp. 151–176. 2009. <https://doi.org/10.1002/nme.2397>
- [41] Lee, J. Ho, Kim, J. K., Kim, J. H. "Nonlinear analysis of soil-structure interaction using perfectly matched discrete layers." *Computers & Structures*, 142, pp. 28–44. 2014. <https://doi.org/10.1016/j.compstruc.2014.06.002>
- [42] Jeong, C., Seylabi, E. E., Taciroglu, E. "A time-domain substructuring method for dynamic soil structure interaction analysis of arbitrarily shaped foundation systems on heterogeneous media." *ASCE International Workshop on Computing in Civil Engineering*, June 23–25, 2013, Los Angeles, California. <http://dx.doi.org/10.1061/9780784413029.044>
- [43] Guddati, M. N., Tassoulas. J. L. "Continued-fraction absorbing boundary conditions for the wave equation." *Journal of Computational Acoustics*, 8(1), pp. 139–156. 2000. <https://doi.org/10.1142/S0218396X00000091>
- [44] Lee, J. H., Tassoulas, J. L. "Consistent transmitting boundary with continued-fraction absorbing boundary conditions for analysis of soil-structure interaction in a layered half-space." *Computer Methods in Applied Mechanics and Engineering*, 200(13–16), pp. 1509–1525. 2011. <https://doi.org/10.1016/j.cma.2011.01.004>
- [45] Power, M. S., Rosidi, D., Kaneshiro, J. "Vol. III Strawman screening, evaluation, and retrofit design of tunnels." *Report Draft. National Center for Earthquake Engineering Research*, Buffalo, New York. 1996.
- [46] St John, C. M., Zahrah, T. F. "Aseismic design of underground structures." *Tunnelling and underground space technology*, 2(2), pp. 165–197. 1987. [https://doi.org/10.1016/0886-7798\(87\)90011-3](https://doi.org/10.1016/0886-7798(87)90011-3)
- [47] Hashash, Y. M.A., Hook, J. J., Schmidt, B., Yao, J. I-C. "Seismic design and analysis of underground structures." *Tunnelling and Underground Space Technology*, 16(4), pp. 247–293. 2001. [https://doi.org/10.1016/S0886-7798\(01\)00051-7](https://doi.org/10.1016/S0886-7798(01)00051-7)
- [48] American Lifelines Alliance (ALA). "Seismic Guidelines for Water Pipelines". 2005. [https://www.americanlifelinesalliance.com/pdf/SeismicGuidelines\\_WaterPipelines\\_PL.pdf](https://www.americanlifelinesalliance.com/pdf/SeismicGuidelines_WaterPipelines_PL.pdf)
- [49] Newmark, N. M., Rosenblueth, E. "Fundamentals of earthquake engineering." *Civil Engineering and Engineering Mechanics series 12. p. 640. 1971*.

- [50] O'Rourke, M. J., Liu, X. "Response of buried pipelines subject to earthquake effects." MCEER Monograph No. 3. 1999. <http://mceer.buffalo.edu/publications/monographs/99-MN03.pdf>
- [51] Roudsari, M. T. (2011). "Using neural network for reliability assessment of buried pipelines subjected of earthquake." Ph.D. thesis, *Science and Research Branch of the Islamic Azad University Tehran, Iran.*
- [52] ABAQUS [Computer software]. *Hibbitt, Karlsson, & Sorensen.*
- [53] Uniform Building Code. 1994. [digitalassets.lib.berkeley.edu/ubc/UBC\\_1994\\_v2.pdf](http://digitalassets.lib.berkeley.edu/ubc/UBC_1994_v2.pdf)